Visible Light Absorption by Various Titanium Dioxide Specimens†

Vyacheslav N. Kuznetsov‡ and Nick Serpone*,§

Fock Research Institute of Physics, St. Petersburg State University, Ulyanovskaya St. 1, St. Petersburg 198504, Russia, and Dipartimento di Chimica Organica, Universita di Pavia, Via Taramelli 10, Pavia 27100, Italy

Received: July 6, 2006; In Final Form: August 14, 2006

A set of heat-induced and photoinduced absorption spectra of various compositions of Degussa P25 TiO_2 and different polymers has been examined. The spectra are described as the sum of overlapping absorption bands (ABs) with maxima at 2.90 eV (427 nm, AB1), 2.55 eV (486 nm, AB2), and 2.05 eV (604 nm, AB3); the spectra correlate entirely with the experimentally observed absorption spectra after the reduction of TiO_2. Absorption spectra of visible-light-active TiO_2 photocatalysts reported recently in the literature have also been analyzed. Relatively narrow absorption spectra are very similar and independent of the method of photocatalyst preparation. The average absorption spectrum can be described reasonably well by the sum of the two absorption bands AB1 and AB2. It is argued that visible light activation of TiO_2 specimens (anion-doped or otherwise) implicates defects associated with oxygen vacancies that give rise to color centers displaying these absorption bands and not to a narrowing of the original band gap of TiO_2 ($E_{BG} \approx 3.2$ eV, anatase) through mixing of dopant and oxygen states, as has been suggested recently in the literature.

1. Introduction

The past decade has witnessed extensive efforts expended to develop TiO_2 specimens with high visible light activity (VLA) in photocatalytic reactions. Titanium dioxide has been treated with hydrogen plasma at elevated temperatures[1] and doped with different transition metal ions[2,3] and with different anions (N, F, S) that replace oxygen in the crystal lattice.[4−7] Anion doping has attracted much interest because it can be achieved successfully at relatively low temperatures.[4] Typically, visible light absorption and the VLA of anion-doped TiO_2 have been ascribed to the narrowing of the band gap that might result from mixing anion and oxygen states.[4] Concomitantly, from their studies Ihara and co-workers concluded that oxygen-deficient sites play an important role in the origin of the VLA of TiO_2 specimens for both H_2-plasma-treated TiO_2[1] and N-doped TiO_2.[8] The appearance of VLA for F-doped TiO_2[9] and S-doped TiO_2[7] has also been attributed to the generation of oxygen vacancies. By contrast, using photoluminescence and electron paramagnetic resonance techniques Prokes and co-workers[10] attributed the visible light absorption of their titania-based oxinitride to an oxygen hole center (OHC), namely, $Ti^{IV}-O-Ti^{IV}-O^{\bullet}$, created near the surface of the nanocolloid. They further proposed that the energy level of this OHC defect was within the band gap of the TiO_2 and was associated neither with the conduction band nor with the valence band of TiO_2. In many cases, the origin of the visible light absorption (and also VLA) resulting from incorporation of transition metal ions into the TiO_2 network has been connected with the formation of new energy levels within the forbidden energy gap of the semiconductor material.[3] The VLA of metal oxides induced by metal-ion implantation has been associated by Anpo and Takeuchi[2] to long-distance interactions between the metal oxide TiO_2 and the metal-ion dopants. Clearly, there are various discrepant interpretations of the absorption features in the same spectral range for doped TiO_2 systems.

Comparison of the absorption spectra of different types of visible-light-active TiO_2 samples is a rather difficult task because the bandwidths of the spectral band(s) may depend significantly on the preparative method(s). Nevertheless, for relatively narrow absorption spectra in the range of 400−600 nm (i.e., 3.10−2.07 eV) even a simple visual comparison gives considerable evidence of the similarities between the spectra. It is reasonable then to query whether such spectral similarities are accidental or whether they have any physical cause or reason.

The aim of this study was to investigate TiO_2 absorption spectra in the visible light region. In our earlier study of the diffuse reflectance spectra (DRS's) of powdered compositions of TiO_2/polymers, we reported that light absorption by these systems originated (i) only in the visible spectral region and (ii) after subjecting them to a relatively low-temperature heat treatment above 350 K.[11] Comparison of the absorption spectra of such compositions with spectra of powdered samples of TiO_2 reduced in H_2 or CO environments[12] permitted assignments of the absorption features to defects associated with oxygen vacancies in TiO_2. It is relevant to note that TiO_2 reduced in the presence of polymeric materials exhibits a set of related absorption spectra that appreciably simplifies data numerical analysis.

2. Experimental Section

Commercially available Degussa P25 titanium dioxide (ca. 80% anatase, 20% rutile) was calcined in air at 600 K for 5 h to eliminate any adsorbed/absorbed organic impurities. The powdered TiO_2 samples (200 mg) were placed in a 30 mm diameter stainless steel dish (4 mm deep) and were then impregnated with an acetone solution of the polymer (loading, 10−30 mg mL^{-1} of solution). After being dried, the composi-

† Part of the special issue "Arthur J. Nozik Festschrift".

* Author to whom correspondence should be addressed. E-mail: nick.serpone@unipv.it or nickser@alcor.concordia.ca.

‡ St. Petersburg State University.

§ Universita di Pavia.

10.1021/jp064253b CCC: $33.50
Published on Web 09/21/2006

tions contained 10−20 wt % of the polymer. Samples were kept in the dark prior to and between the heat or irradiation treatments and the optical measurements.

In the present study, polymers with different monomeric units and structures were used: Poly(vinylidene fluoride/*co*-hexafluoropropylene) (P(VDF−HFP)) and poly(vinylidene fluoride/*co*-tetrafluoroethylene) (P(VDF−TFE)) were selected as the fluoropolymers, whereas polymethylphenylsiloxane (PMPS) was the representative of the class of polysiloxanes. Monomeric units of polyvinylbutyral (PVB) and poly(ethylmethacrylate/*co*-methylacrylate) (P(EMA−MA)) included C, H, and O atoms and comprised different pendant (side) groups. We hasten to emphasize that in the present context the polymers acted only as the reactive organic media. That is, the polymers undergo either oxidative photodegradation or thermal degradation in the presence of TiO_2 depending on the conditions used.[11] The absence of a (photo or thermal) treatment-induced absorption in control samples of the polymers and the TiO_2 specimens (see below) infers that the TiO_2/polymer compositions thermally or photodegrade on interaction of the polymers with the metal oxide. In this regard, three principal properties connect the selected polymers: (a) their transparency in the visible spectral region, (b) their relatively high thermal stability and photostability, and (c) their solubility in the same solvent medium (acetone).

UV−vis DRS's were measured on a Beckman UV-5270 spectrophotometer equipped with an integrating sphere assembly that used $BaSO_4$ as the reference standard. Difference DRS spectra ($\Delta\rho$) were plotted to demonstrate the spectral changes in the reflectivity (absorption enhancement). If $\rho_1(h\nu)$ and $\rho_2(h\nu)$ are the DRS spectra measured *before* and *after* the sample treatment (heat or irradiation), respectively, then the difference $\{\rho_1(h\nu) - \rho_2(h\nu)\} > 0$, that is $\Delta\rho(h\nu) > 0$, corresponds to the treatment-induced absorption spectrum. Further details regarding the DRS analysis are available elsewhere.[11]

Samples of the TiO_2/polymer compositions were either heat-treated in air (a) at the desired temperatures for a given time period or (b) at a constant rate $\beta = 0.1$ K s^{-1} as per the law $T = T_0 + \beta t$, where T_0 is ambient temperature (programmed heating) and t is time. The computer-controlled temperature-programmed heating procedure was accompanied by the *simultaneous* measurement of the temperature dependence of the diffuse reflectance at a desired wavelength (ρ_λ).[13] The procedure provided a measurement accuracy of $\delta\rho/\rho \leq 0.1\%$ and permitted treatment of the data in the differential form $d\Delta\rho_\lambda/dt$ or $d\Delta\rho_\lambda/dT$, which has proven convenient for numerical analysis.

Samples of the TiO_2/polymer compositions were irradiated in air or under a nitrogen atmosphere using a set of four commercially available 20 W fluorescent lamps located at a distance of 80 mm from the samples. The spectrum of the lamps consisted of a quasi-continuous fluorescent emission in the visible region along with the usual Hg lines at ≥365 nm that accounted for less than ca. 3% of the total light flux.[14] To control the thermal and photostability of the polymers, films were also prepared (no TiO_2) from an acetone solution in a dish made of polished aluminum. The thickness of the films was about 1 mm. They were heat-treated or irradiated simultaneously with the TiO_2/polymer compositions. Changes in the DRS's of such samples provided information on any changes in the color of the polymer films.

3. Results and Discussion

3.1. Spectral Features of TiO_2/Polymer Compositions. Each TiO_2/polymer composition exhibited absorption features in the spectral range of 3.1−1.8 eV (400−700 nm) when heated at a temperature above 340 K. The DRS's ($\rho(h\nu)$) of the TiO_2/P(VDF−HFP) and TiO_2/PVB compositions are displayed in Figure 1, which exhibits very similar spectra (spectra 3 and 4) after heating the compositions at 360 K for 3 h. Usage of difference spectra $\Delta\rho(h\nu)$ (spectra 3a and 4a) allows for the characterization of each absorption spectrum by the position of the spectral maximum ($h\nu_{max}$), the intensity of this maximum ($\Delta\rho_{max}$), and the spectral bandwidth at half-maximum amplitude ($\delta h\nu_{1/2}$). After a heat treatment at 450 K for 3 h, the polymer films (free of titania) exhibited negligible changes in the DRS's. Consequently, the absorption spectral features induced by the heat treatment of TiO_2/polymer compositions resulted from the reaction between the macromolecules and TiO_2.

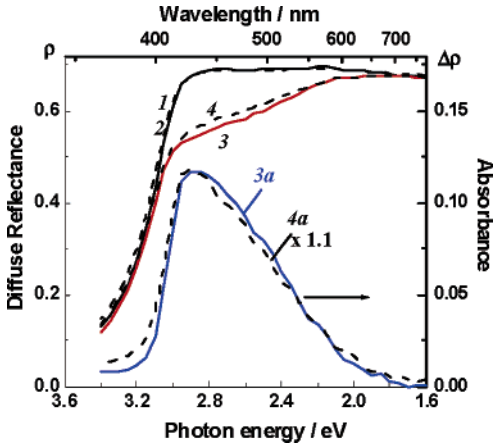

Figure 1. DRS's of TiO_2/P(VDF−HFP) (ρ, spectra 1 and 3) and TiO_2/PVB (spectra 2 and 4) compositions, *before* (spectra 1 and 2) and *after* (spectra 3 and 4) heating at 360 K for 3 h. Curves 3a and 4a are absorption spectra (i.e., difference DRS's, $\Delta\rho$): Spectrum 3a was obtained as spectrum 1 minus spectrum 3, whereas absorption spectrum 4a is spectrum 2 minus spectrum 4.

Three main features of the heat-induced absorption spectra of the titania/polymer compositions are worth noting: (i) the dependence of $\Delta\rho_{max}$ on the temperature of the heat treatment or the heating time at a given temperature for each composition, (ii) the independence of $h\nu_{max}$ and $\delta h\nu_{1/2}$ on the type of polymer substrate used for comparable $\Delta\rho_{max}$ values (similarity of spectra, e.g., spectra 3a and 4a in Figure 1), and (iii) the increase of $\delta h\nu_{1/2}$ (i.e., broadening of the spectra) with the increase in $\Delta\rho_{max}$.

The similarity of the absorption spectra allows for the averaging of spectra of the different compositions when $\Delta\rho_{max}$ values do not differ greatly. For comparison, the spectra with $\Delta\rho_{max}$ lying in a finite range were normalized by $\Delta\rho_{max}$ and subsequently averaged. Figure 2 illustrates the resulting spectra for three different values of $\Delta\rho_{max}$: 0.04 ± 0.01 (spectrum 1), 0.10 ± 0.01 (spectrum 2), and 0.19 ± 0.01 (spectrum 3). Accordingly, a set of gradually changing and closely related absorption spectra were obtained for examination.

Broadening of the spectra illustrated in Figure 2 implies that the spectra consist of a few overlapping absorption bands (ABs) and that the contribution of long-wavelength bands increases with an increase in $\Delta\rho_{max}$. The number of individual AB bands was determined using the Alentsev−Fock method[15] based on the calculation of differences of the experimental spectra in which the contribution of all the bands, except one, is minimized. The three bands with $h\nu_{max}$ at about 2.90, 2.55, and 2.05 eV were thus obtained by this method. Additionally, analysis of spectra 1, 2, and 3 in Figure 2 showed that each spectrum can be described reasonably well by the sum of three Gaussian absorption bands with $h\nu_{max}$ for AB1 at 2.90 ± 0.01 eV, for

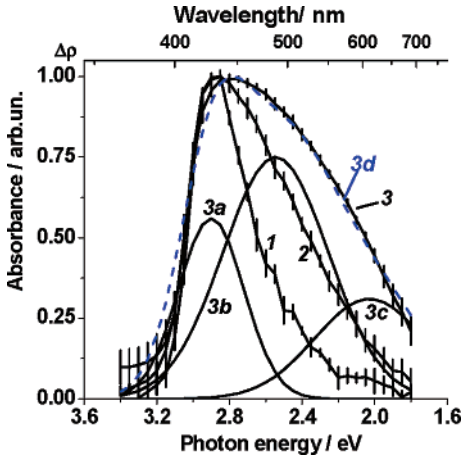

Figure 2. Averaged absorption spectra ($\Delta\rho$) of various TiO_2/polymer compositions normalized by $\Delta\rho_{max}$ for $\Delta\rho_{max} = 0.04 \pm 0.01$ (spectrum 1), 0.10 ± 0.01 (spectrum 2), and 0.19 ± 0.01 (spectrum 3). Deconvolution of the experimental absorption spectrum 3 into three Gaussian ABs (spectra 3a, 3b, and 3c). Spectrum 3d represents the sum of the three absorption bands 3a, 3b, and 3c. Error bars in all the absorption spectra represent the uncertainty in the averaged spectra.

AB2 at 2.55 ± 0.05 eV, and for AB3 at 2.05 ± 0.01 eV. The relevant $\delta h\nu_{1/2}$ value for AB1 is 0.35 ± 0.01 eV, for AB2 it is 0.54 ± 0.02 eV, and for AB3 it is 0.55 ± 0.02 eV. The relative band intensities $\Delta\rho_{max}$ are AB1/AB2/AB3 = 0.80:0.18:0.02 (spectrum 1), 0.52:0.42:0.06 (spectrum 2), and 0.35:0.46:0.19 (spectrum 3); see also the Table 1 footnotes. The characteristics of the three Gaussian absorption bands resulting from the deconvolution of the normalized averaged absorption spectra of Figure 2 for the TiO_2/polymer compositions (spectra 1, 2, and 3) are summarized in Table 1. It is evident that spectral broadening results from an increase of the relative contributions of the AB2 and AB3 bands. The Gaussian absorption bands 3a, 3b, and 3c, and their sum 3d, which accords with absorption spectrum 3, are also illustrated in Figure 2.

The possible temperature dependence of the absorption intensity at a given wavelength ($\Delta\rho_\lambda$) near the fundamental absorption edge for TiO_2 ($h\nu \leq 3.2$ eV; Degussa P25) was examined earlier[11] on the notion that the reflectance (ρ_λ) of a metal oxide at that wavelength can change not only as a result of an increase in the absorption band intensity but potentially also as a result of thermal displacement of the absorption edge. Contrary to ZnO, however, this displacement appears rather insignificant for TiO_2.[11] Features emanating from the interactions of P25 TiO_2 with polymers of various types are clearly seen from the temperature dependences of the heat-induced absorption growth displayed in Figure 3. The dependences $\Delta\rho_\lambda(T)$ of the compositions subjected to the heat treatment at a constant heating rate of 0.1 K s^{-1} were measured near the maximum at 470 nm ($h\nu = 2.64$ eV) in the absorption spectra of Figure 2 to minimize the influence of any thermal displacement that might occur. Figure 3 also illustrates the variations in the rates of increase of the absorbance showing a strong dependence on the nature of the polymer used.

Figure 4 depicts the temperature dependences in Arrhenius coordinates, which allow for an estimate of the activation energies of the absorbance growth. During the initial stages of the absorption growth at the lower temperatures, changes in the concentrations of the polymers that take an active part in the reaction are insignificant so that the rate of reaction is independent of *reactant* concentration. Accordingly, activation energies can be calculated directly from the slopes of the linear dependences from plots of $\ln(d\Delta\rho_\lambda/dt)$ versus $1/kT$, where k is Boltzmann's constant. Activation energies lie in a wide energy range from 0.14 eV for P(EMA−MA) (Figure 4, curve 1) to 0.8−1.0 eV for the fluoropolymers (Figure 4, curves 4 and 5). Considering the shape (form) of the absorption spectra as being independent of the TiO_2/polymer compositions, as demonstrated by the spectra 3a and 4a of Figure 1 and as mentioned above, the temperature dependences reported in Figures 3 and 4 must then reflect variations in the thermal formation of the color centers. Indeed, contrary to the absorption spectra of the color centers, the rates and the activation energies of formation of color centers in TiO_2 depend strongly on the type of polymer used as the *reactant*. It should be understood that the term *type of polymer* includes not only the characteristics of the macromolecules such as content and structure (among others) but also the morphology of the polymers (degree of crystallinity and defect bonds, among others). Clearly, different properties can govern the activity of the polymers in the reduction of TiO_2. A detailed investigation of the reaction mechanisms for each of the TiO_2/polymer compositions was not the aim of the present study.

The kinetics of the increase in absorbance measured at $\lambda = 430$ nm ($h\nu = 2.88$ eV) for TiO_2/polymer compositions under irradiation emitted by the fluorescent lamps (see above) show that the spectral range of irradiation (either by UV only or by the full spectrum of the lamps) and the nature of the atmospheres (air under normal conditions or dry nitrogen) have a noticeable effect (about ±20−30%) on the rates of the absorbance growth. The principal differences in the rates of photocoloration, however, arise from the type of polymer used. For instance, in all the experiments performed the rates of photocoloration of TiO_2 followed the same sequence relative to the nature of the polymer in the compositions: PMPS (1.0) > PVB (0.6) > P(EMA−MA) (0.4) > P(VDF−HFP) (0.15). The values in parentheses indicate the normalized increase of the absorbance at $\lambda = 430$ nm after irradiation for 4.5 h. At the same time, TiO_2-free polymer films exhibited negligible changes in the DRS's even after prolonged irradiation (ca. 25 h). Note that the above sequence differs greatly from the sequence that is evident in Figure 3: P(VDF−TFE) > P(VDF−HFP) > PVB > PMPS > P(EMA−MA). Accordingly, results on the photodegradation and the thermal degradation of the TiO_2/polymer compositions clearly indicate the existence of some differences in the pathways of formation of the *same* color centers in titania that are responsible for the light absorption in the visible spectral region. In the latter case, thermal degradation will be governed by the chemical changes in the surface complexes (adsorbates) between the macromolecules and the surface atoms of the metal oxide.[11] That is, thermal activation of the adsorbates can cause weakening of the bonds in the macromolecules with subsequent transfer of some pertinent atoms to the metal-oxide surface, ultimately leading to formation of oxygen vacancies and to the corresponding color centers. By contrast, photocoloration of the metal oxide TiO_2 in polymer/TiO_2 compositions typically takes place by photoactivation of the TiO_2 with subsequent generation of reducing and oxidizing equivalents (electrons and holes) followed by oxidative degradation of the polymeric adsorbate by the latter[16] and ultimate trapping of electrons by the anion vacancies (V_a) to yield F-type centers.[17]

The averaged absorption spectra (curves 1) illustrating the photostimulated coloration (i.e., formation of color centers) of titania for the compositions with the PMPS, PVB, P(EMA−MA), and P(VDF−HFP) polymers after irradiation of the compositions in air (Figure 5a) and under a nitrogen atmosphere (Figure 5b) are displayed in Figure 5.

TABLE 1: Characteristics of the Gaussian Absorption Bands in the Analysis of the Absorption Spectra of Various TiO_2/Polymer Compositions

AB1,[a] $h\nu_{max}$ (eV)	AB1 $\delta h\nu_{1/2}$ (eV)	AB1[b] relative I (%)	AB2 $h\nu_{max}$ (eV)	AB2 $\delta h\nu_{1/2}$ (eV)	AB2 relative I (%)	AB3 $h\nu_{max}$ (eV)	AB3 $\delta h\nu_{1/2}$ (eV)	AB3 relative I (%)	figure
2.90	0.36	80	2.55	0.48	18	2.03	0.60	2	Figure 2, spectrum 1
2.90	0.36	52	2.55	0.53	42	2.03	0.60	6	Figure 2, spectrum 2
2.90	0.36	35	2.55	0.58	46	2.03	0.60	19	Figure 2, spectrum 3
2.90	0.35	74	2.56	0.51	21	2.05	0.52	4	Figure 5a
2.91	0.35	55	2.56	0.51	42	2.05	0.52	3	Figure 5b

[a] AB1 denotes spectrum 3a, AB2 denotes spectrum 3b, and AB3 represents spectrum 3c in Figure 2. In Figure 5, the AB1, AB2, and AB3 bands correspond, respectively, to spectra 1a, 1b, and 1c. [b] The sum of the relative intensities in any one row equals 100%.

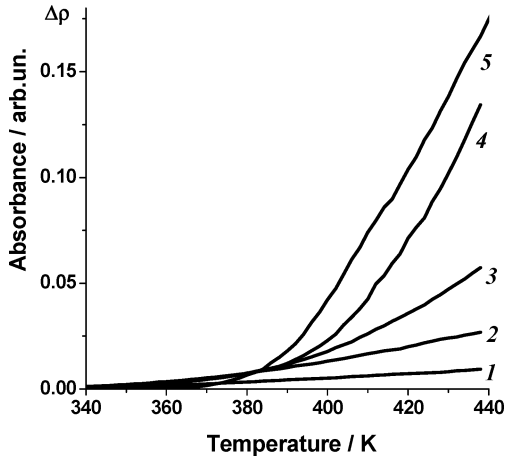

Figure 3. Temperature dependences of the absorbance ($\Delta\rho_\lambda$) at λ = 470 nm induced in the compositions consisting of TiO_2 and P(EMA−MA) (curve 1), PMPS (curve 2), PVB (curve 3), P(VDF−HFP) (curve 4), and P(VDF−TFE) (curve 5) under a temperature programmed heat treatment at a constant heating rate of 0.1 K s^{-1} in air.

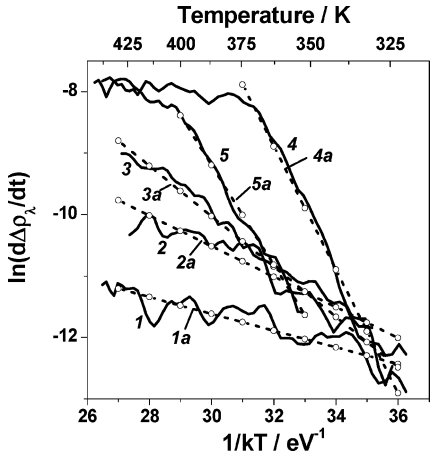

Figure 4. Temperature dependences of the rate of absorbance growth at λ = 470 nm ($d\Delta\rho_\lambda/dt$) in the Arrhenius coordinates for compositions consisting of TiO_2 and P(EMA−MA) (curve 1), PMPS (curve 2), PVB (curve 3), P(VDF−HFP) (curve 4), and P(VDF−TFE) (curve 5). Lines 1a through 5a are linear fits of the calculated curves.

The spectra whose characteristics ($h\nu_{max}$, $\delta h\nu_{1/2}$, and relative intensity I) are summarized in the last two rows of Table 1 could also be deconvoluted by three Gaussian absorption bands. The goodness of the fitting procedure is indicated by the sum of the three absorption bands 1a−c yielding spectra 1d, in good accord with the averaged experimental spectra 1**.** The data of Table 1 clearly show that in all cases the absorption spectra are the sum of the same (identical) overlapping absorption bands. Note that obtaining such reliable data becomes possible only when using a set of related absorption spectra of the TiO_2/polymer compositions.

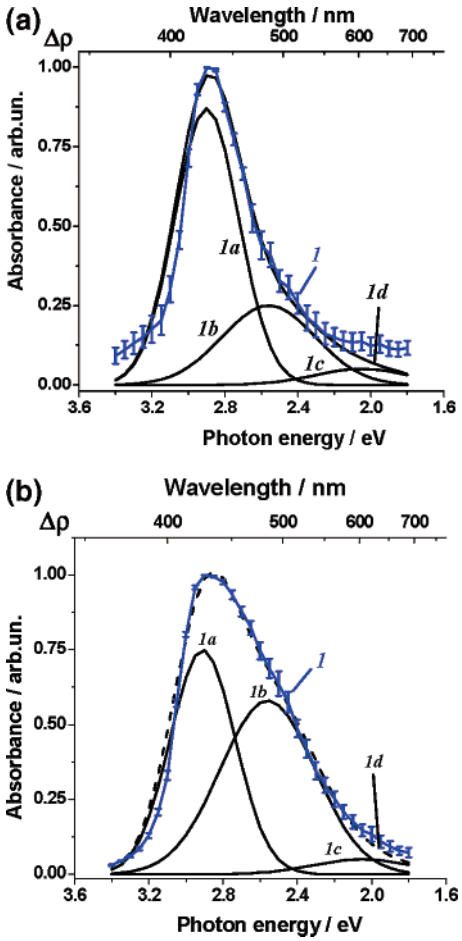

Figure 5. Averaged absorption spectra $\Delta\rho$ (1) of various TiO_2/polymer compositions normalized by $\Delta\rho_{max}$. Deconvolution of the experimental absorption spectrum into three Gaussian absorption bands (spectra 1a, 1b, and 1c). Spectrum 1d represents the sum of the three absorption bands 1a, 1b, and 1c. Absorption was induced by fluorescent lamp irradiation for 4.5 h (a) in air with relative humidity ca. 20% or (b) under a N_2 atmosphere with relative humidity ca. 2%.

The spectra of P25 TiO_2 reduced under conditions that greatly differ from those used in this work, such as TiO_2 being calcined in a H_2 or CO atmosphere at temperatures $T \geq 700$ K and then bleached in the presence of O_2, N_2O, or NO, can also be described by the sum of three Gaussian absorption bands with $h\nu_{max}$ for AB1 at 2.81 ± 0.01 eV, for AB2 at 2.55 ± 0.01 eV, and for AB3 at 2.00 ± 0.02 eV.[18]

The independence of $h\nu_{max}$ and $\delta h\nu_{1/2}$ of the absorption bands in the spectra of the TiO_2/polymer compositions on the type of polymeric material and the absence of recognizable differences between the parameters of the absorption band obtained in this work (Table 1) and in the study of Lisachenko and coworkers[18] indicate unambiguously (i) that structural defects (i.e., color

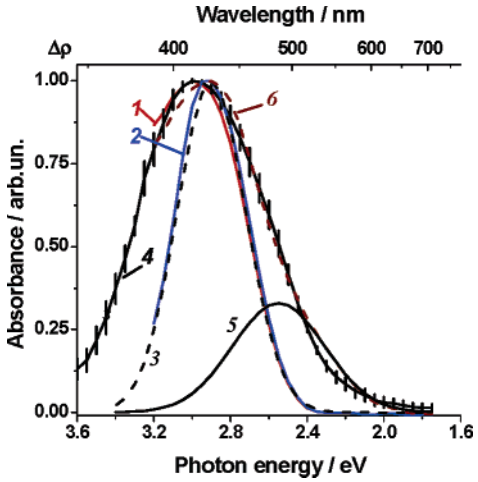

Figure 6. Spectrum 1, the absorption spectrum of the color centers in the anatase crystal reported by Sekiya and co-workers;[19] spectrum 2, spectrum 1 multiplied by the reflectance spectrum of P25 TiO_2; spectrum 3, the Gaussian AB1; spectrum 4, the mean absorption spectrum of the visible-light-active TiO_2; spectrum 5, the Gaussian AB2; spectrum 6, fitting of spectrum 4 (see text).

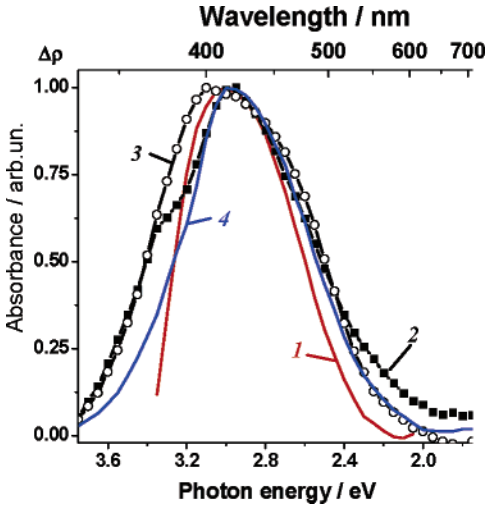

Figure 7. Difference DRS's (absorption spectra) of various anion-doped titania specimens: spectrum 1, N/F-doped TiO_2; spectrum 2, N-doped anatase TiO_2; spectrum 3, N-doped rutile TiO_2; and spectrum 4, yellow nitrided $TiO_{2-x}N_x$ nanocolloids.

centers) responsible for these bands exist in the solid TiO_2 specimens and (ii) that these color centers are associated with the reduction of TiO_2.

We now compare the absorption bands obtained by the deconvolution techniques with the experimental absorption spectra of color centers in TiO_2. At present, well-resolved spectra have been reported only for anatase single crystals.[19] The difference in the absorption spectra of yellow and colorless TiO_2 crystals reported by Sekiya and co-workers[19] is displayed in Figure 6 (spectrum 1).

To take into account the difference(s) of the optical properties near the band gap absorption edge (3.1−3.2 eV) of anatase crystals and powdered P25 TiO_2, spectrum 1 was multiplied by the DRS spectrum of P25 TiO_2. The resulting spectrum 2 in Figure 6 overlaps completely with the absorption band AB1 (spectrum 3). To the extent that the absorption band at 3.0 eV is associated with oxygen vacancies,[19] the congruence of spectra 2 and 3 can be taken as independent evidence of the validity of the proposed interpretation of the TiO_2 absorption spectra.

3.2. Spectral Features of Visible-Light-Active TiO_2. A few absorption spectra have been selected for numerical analysis to evaluate the inherent similarities among the spectral characteristics of titania samples. The analysis included digitization (numbering) of the DRS's of the sample in non-visible-light-active and visible-light-active states, calculation of the difference between these DRS's, and the normalization of the spectra by the $\Delta\rho_{max}$ factor. Results of the analysis show that relatively narrow absorption spectra ($\delta h\nu_{1/2} \approx 0.6$ eV) are indeed very similar and independent of the methods of preparation of these visible-light-active TiO_2 specimens. The spectral similarity affords a calculation of the average spectrum of the visible-light-active TiO_2 sample with standard error ca. $\leq$5% (Figure 6, spectrum 4). Note that the averaged spectrum 4 was obtained by averaging the absorption spectra of Cr-implanted TiO_2,[2] Ce-doped TiO_2,[3] mechanochemically activated N-doped TiO_2,[5] N-doped oxygen-deficient TiO_2,[8] and $Sr_{0.95}La_{0.05}TiO_{3+\delta}$ treated with HNO_3 acid.[20]

The mean spectrum 4 of visible-light-active TiO_2 in Figure 6 was fitted using the absorption band at 3.00 eV from the work of Sekiya et al.[19] and the Gaussian absorption band AB2 with $h\nu_{max} = 2.55$ eV and $\delta h\nu_{1/2} = 0.50$ eV (Figure 6, spectrum 5). The resulting spectrum 6 of Figure 6 clearly shows that the absorption spectrum of visible-light-active TiO_2 consists of absorption bands AB1 (spectrum 3 of Figure 6) and AB2 (spectrum 5 of Figure 6) with relative intensities AB1/AB2 = 0.74:0.26. Concomitantly, several visible-light-active TiO_2 specimens (e.g., the work of Ihara and co-workers[1]) and reduced TiO_2, in general, exhibit broad and poorly resolved absorption spectra relative to spectrum 4 of Figure 6. After reduction in a H_2 atmosphere at ~970 K, rutile TiO_2 crystals displayed very broad absorption spectra from about 3.0 to 0.1 eV with maxima at 0.75 and 1.18 eV.[21] Poor spectral resolution and wide spectral bandwidths result from a variety of coexisting *intrinsic* bulk and surface defects/color centers, both in crystals and in powdered TiO_2 specimens. The principal defects have been identified as neutral, singly, and doubly charged oxygen vacancies and trivalent and tetravalent Ti interstitials in different structural positions.[22] Nonetheless, despite years of studies, resolution of the individual absorption bands and reliable assignments of these bands to color centers in reduced TiO_2 are still the subject of some debate.

On the basis of the above discussion, representation of the TiO_2 absorption spectra in the visible region as the sum of overlapping absorption bands stimulates an analysis of the known absorption spectra of the VLA of TiO_2 photocatalysts. As noted earlier, such spectra often show strong similarities. For instance, Figure 7 illustrates the difference DRS's ($\Delta\rho$, synonymous with absorption spectra) of (i) a N/F-doped TiO_2 sample (spectrum 1) prepared by a spray pyrolytic method,[23] (ii) a N-doped *anatase* TiO_2 specimen (spectrum 2) and a N-doped *rutile* TiO_2 sample (spectrum 3) prepared by a solvothermal process,[24] and (iii) a yellow N-doped TiO_2 system (spectrum 4) synthesized in short time at ambient temperatures using a nanoscale exclusive direct nitridation of TiO_2 nanocolloids with alkylammonium compounds.[25] It is also a remarkable observation that the absorption spectra of the nitride $TiO_{2-x}N_x$ nanocolloids are independent of the crystalline phase (anatase versus rutile) of the titania specimens. Accordingly, the absorption bands comprised in the spectra of the color centers must also be independent of the phase composition of the titania specimens.

Figure 8 reports the absorption spectra of two cation-doped TiO_2 specimens: (i) Fe-doped TiO_2 nanopowders (spectrum 1) prepared by oxidative pyrolysis of organometallic precursors in an induction thermal plasma reactor[26] and (ii) zinc-ferrite-

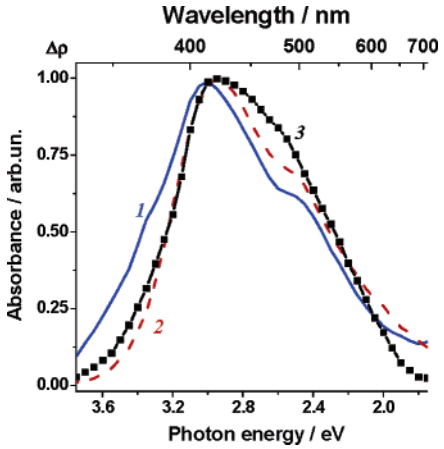

Figure 8. Absorption spectra ($\Delta\rho$) of Fe-doped TiO_2 (spectrum 1), TiO_2 doped with zinc ferrite (spectrum 2), and orange nitrided large $TiO_{2-x}N_x$ clusters (spectrum 3; compare with spectrum 4 of Figure 7 for yellow nitrided nanocolloids).

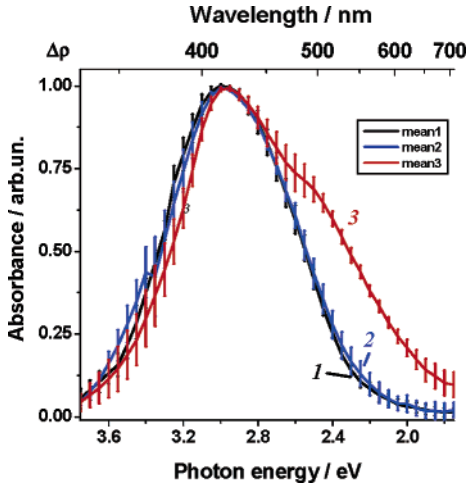

Figure 9. Average absorption spectra ($\Delta\rho$) of various titania systems. Spectrum 1, same as spectrum 4 of Figure 6 (see text for details); spectrum 2, anion-doped TiO_2 specimens (Figure 7); and spectrum 3, cation-doped TiO_2 samples (Figure 8).

doped titania ($TiO_2/ZnFe_2O_4$, spectrum 2) synthesized by sol−gel methods followed by calcinations at various temperatures.[27] Also shown is the spectrum of the orange N-doped TiO_2 sample (spectrum 3) prepared by a procedure otherwise identical to that of yellow N-doped TiO_2 but with the former consisting of partially agglomerated nanocolloids, that is larger $TiO_{2-x}N_x$ clusters.[25] In some cases, the absorption spectra of visible-light-active TiO_2 systems show clear shoulders for some doped titanium oxides, which are seen on the low-energy side at ca. 2.5 eV (spectra 1, 2, and 3 in Figure 8).

The average absorption spectra of anion-doped and cation-doped titanias are displayed in Figure 9. Spectrum 1 is the mean spectrum 4 in Figure 6 reported here for comparison, spectrum 2 is the average spectrum obtained by averaging the spectra reported in Figure 7, and spectrum 3 represents the average spectrum obtained by averaging the spectra illustrated in Figure 8. Clearly, the remarkable overlap of the relatively narrow average spectra 1 and 2 in Figure 9 emphasizes once more the independence of the spectra on the method of photocatalyst preparation and appears to be a general feature of the electronic and spectral features of the color centers/defects of TiO_2. A comparison of the broader mean spectrum 3 in Figure 9 with the narrower spectra 1 and 2 indicates that broadening of the absorption spectrum of TiO_2 photocatalysts originates from the long-wavelength absorption band, in this case the AB2 band. This assertion requires no spectral deconvolution.

3.3. Causes for the Similarities in Absorption Features. The broad absorption spectra of P25 TiO_2 reduced in a H_2 or CO atmosphere display one maximum at 1.24 eV in the spectral range from 3.0 to 0.5 eV.[12,18] However, irreversible adsorption of O_2, NO, and N_2O at ambient temperatures[12,18,28,29] decreases the absorption mostly in the long-wavelength region. Adsorption of molecular O_2 on TiO_2 affects light absorption rather effectively such that the absorption bands AB1 and AB2 become prominent.[12,18] Bleaching of H_2 heat-treated TiO_2 specimens by air addition was also observed in the work of Ihara and coworkers.[1] Hence, among the above-mentioned color centers, only those centers that are slightly active interact with oxygen and predominate in the presence of O_2. This result explains why TiO_2 reduction can take place in air and why the absorption spectra of such TiO_2 specimens consist mainly of the short-wavelength absorption bands AB1 and AB2; see, for example, Figures 2, 5, and 6.

The coincidence of the absorption bands in the visible spectral region for reduced TiO_2 (this work and the studies by Kuznetsov and Krutitskaya,[12] Lisachenko et al.,[18] and Sekiya et al.[19]) with those of visible-light-active TiO_2 samples indicates that the processes involved in the preparation of visible-light-active TiO_2 specimens (irrespective of the method) also implicate a stage of TiO_2 reduction. Demonstrating this stage and its mechanism, however, constitute separate problems and are not dealt with here. All the preparative methods include a heating stage, although the heating temperatures differ noticeably. For instance, the absorption band that appears at 3.0 eV in anatase crystals and that has been attributed to oxygen vacancies results from the removal of impurities introduced (perhaps inadvertently) during the crystal growth at 570 K.[19] The temperature dependences of the absorption at 2.88 eV of N-doped TiO_2 and the corresponding VLA of TiO_2 in the photooxidation of acetone on calcination temperatures correlate completely, a correlation that displays a common maximum at 670 K.[8] Related to this, the visible light absorption of metal-ion-implanted TiO_2 systems reported by Anpo and Takeuchi[2] was observed only after the samples had been calcined in the temperature range between 723 and 823 K.

4. Concluding Remarks

Characterization of TiO_2 reduced in polymeric media using absorption spectra (equivalent to difference DRS's) has revealed that a set of absorption spectra can be represented as the sum of individual Gaussian absorption bands with maxima at about 2.90 eV (AB1), 2.55 eV (AB2), and 2.05 eV (AB3). No large changes were seen in the spectral positions and bandwidths at half-maximum amplitudes of the absorption bands of TiO_2 reduced in organic media, when compared to TiO_2 specimens reduced in H_2 or CO environments (after O_2 adsorption only)[12,18] and to reduced anatase crystals.[19] Digitization of DRS's (ρ-($h\nu$)) reported earlier for visible-light-activated TiO_2 systems and calculation of their absorption spectra ($\Delta\rho(h\nu)$) have shown that the relatively narrow spectra bear strong similarities to each other and are independent of the preparation methods of these visible-light-active TiO_2 samples. Their averaged absorption spectra can be described reasonably well by the sum of the two short-wavelength Gaussian absorption bands AB1 and AB2.

It is important to recognize that, in all cases, the absorption features displayed by TiO_2 specimens in the visible spectral region are caused by the formation of color centers that originate from the reduction of TiO_2 after some form of heat treatment

or photostimulation process. Moreover, the absorption spectra of anion-doped (or otherwise) TiO_2 in the visible spectral region likely originate from the existence of such color centers rather than from a narrowing of the original band gap[30] of TiO_2 (E_{BG} = 3.2 eV; anatase) through mixing of oxygen and dopant states, as has been recently claimed in the literature.[4,5,31−33] True narrowing of the original band gap of the metal-oxide semiconductor would necessitate heavy anion or cation doping, which would require high concentrations of the dopants.[34,35] In the latter case, the metal oxide would probably no longer retain its original integrity. Finally, while the absorption bands AB1 and AB2 have been attributed to the formation of defects associated with oxygen vacancies (color centers), the mechanistic details of the photoactivation of TiO_2 by light absorption into these absorption bands have yet to be fully understood.[36]

Acknowledgment. Early work in this area received financial support from the Russian Foundation for Basic Research (to K.V.N.), whereas studies in Pavia have been supported by a grant from the Ministero dell'Istruzione, Universita e Ricerca (to N.S.).

References and Notes

(1) Ihara, T.; Miyoshi, M.; Anpo, M.; Sugihara, S.; Iriyama, Y. *J. Mater. Sci.* **2001**, *36*, 4201.

(2) Anpo, M.; Takeuchi, M. *J. Catal.* **2003**, *216*, 505.

(3) Li, F. B.; Li, X. Z.; Hou, M. F.; Cheah, K. W.; Choy, W. C. H. *Appl. Catal., A* **2005**, *285*, 181.

(4) Yin, S.; Ihara, K.; Aita, Y.; Komatsu, M.; Sato, T. *J. Photochem. Photobiol., A* **2005**, *179*, 105.

(5) Yin, S.; Yamaki, H.; Komatsu, M.; Zhang, Q.; Wang, J.; Tang, Q.; Saito, F.; Sato, T. *J. Mater. Chem.* **2003**, *13*, 2996.

(6) Li, D.; Haneda, H.; Hishita, S.; Ohashi, N. *Mater. Sci. Eng., B* **2005**, *117*, 67.

(7) Colon, G.; Hidalgo, M. C.; Munuera, G.; Ferino, I.; Cutrufello, M. G.; Navio, J. A. *Appl. Catal., B* **2006**, *63*, 45.

(8) Ihara, T.; Miyoshi, M.; Iriyama, Y.; Matsumoto, O.; Sugihara, S. *Appl. Catal., B* **2003**, *42*, 403.

(9) Li, D.; Haneda, H.; Labhsetwar, N. K.; Hishita, S.; Ohashi, N. *Chem. Phys. Lett.* **2005**, *401*, 579.

(10) Prokes, S. M.; Gole, J. L.; Chen, X.; Burda, C.; Carlos, W. E. *Adv. Funct. Mater.* **2005**, *15*, 161.

(11) Kuznetsov, V. N.; Malkin, M. G. *J. Appl. Spectrosc.* **2000**, *67*, 763.

(12) Kuznetsov, V. N.; Krutitskaya, T. K. *Kinet. Catal.* **1996**, *37*, 446.

(13) Kuznetsov, V. N.; Lisachenko, A. A. *J. Appl. Spectrosc.* **1991,** *54*, 176.

(14) Belver, C.; Bellod, R.; Stewart, S. J.; Requejo, F. G.; Fernandez-Garcia, M. *Appl. Catal., B* **2006,** *65*, 309.

(15) Fock M. V. *Proc. Phys. Inst. Acad. Sci. USSR* **1972**, *59*, 3 (in Russian).

(16) (a) Horikoshi, S.; Hidaka, H.; Serpone, N**.** *J. Photochem. Photobiol., A* **2001**, *138*, 69. (b) Horikoshi, S.; Serpone, N.; Yoshizawa, S.; Knowland, J.; Hidaka, H. *J. Photochem. Photobiol., A* **1999,** *120*, 63. (c) Horikoshi, S.; Hidaka, H.; Hisamatsu, Y.; Serpone, N. *Environ. Sci. Technol.* **1998**, *32*, 4010.

(17) (a) Emeline, A. V.; Kataeva, G. V.; Panasuk, A. V.; Ryabchuk, V. K.; Sheremetyeva, N. V.; Serpone, N. *J. Phys. Chem. B* **2005**, *109*, 5175. (b) Emeline, A. V.; Polikhova, S.; Andreev, N.; Ryabchuk, V. K.; Serpone, N. *J. Phys. Chem. B* **2002**, *106*, 5956. (c) Andreev, N. S.; Emeline, A. V.; Khudnev, V. A.; Polikhova, S. A.; Ryabchuk, V. K.; Serpone N. *Chem. Phys. Lett.* **2000**, *325*, 288. (d) Emeline, A. V.; Kataeva, G. V.; Ryabchuk, V. K.; Serpone, N. *J. Phys. Chem. B* **1999**, *103*, 9190. (e) Emeline, A. V.; Kataeva, G. V.; Litke, A. S.; Rudakova, A. F.; Ryabchuck, V. K.; Serpone, N. *Langmuir* **1998**, *14*, 5011.

(18) Lisachenko, A. A.; Kuznetsov, V. N.; Zacharov, M. N.; Michailov, R. V. *Kinet. Catal.* **2004**, *45*, 189.

(19) Sekiya, T.; Ichimura, K.; Igarashi, M.; Kurita, S. *J. Phys. Chem. Solids* **2000,** *61*, 1237.

(20) Otsuka-Yao-Matsuo, S.; Ueda, M. *J. Photochem. Photobiol., A* **2004**, *168*, 1.

(21) Cronemeyer, D. C. *Phys. Rev.* **1959**, *113*, 1222.

(22) Diebold, U. *Surf. Sci. Rep.* **2003**, *48*, 53.

(23) Li, D.; Ohashi, N.; Hishita, S.; Kolodiazhnyi, T.; Haneda, H. *J. Solid State Chem.* **2005**, *178*, 3293.

(24) Aita, Y.; Komatsu, M.; Yin, S.; Sato, T. *J. Solid State Chem.* **2004**, *177*, 3235.

(25) . Gole, J. L.; Stout, J. D.; Burda, C.; Lou, Y.; Chen, X. *J. Phys. Chem. B* **2004**, *108*, 1230. Also see the Web site: http://www.physics.gatech.edu/people/faculty/jgole.html#links.

(26) Wang, X. H.; Li, J.-G.; Kamiyama, H.; Ishigaki, T. *Thin Solid Films* **2006**, *506−507*, 278.

(27) Cheng, P.; Li, W.; Zhou, T.; Jin, Y.; Gu, M. *J. Photochem. Photobiol., A* **2004**, *168*, 97.

(28) Such molecules as O_2, NO, and N_2O are adsorbed rather strongly to TiO_2 through formation of relatively strong bonds with color centers. Such bonding interactions are destroyed by the heat treatment of the metal oxides as demonstrated by thermoprogrammed desorption studies.[18,29]

(29) Kuznetsov, V. N. *Kinet. Catal.* **2002**, *43*, 868.

(30) Serpone N. *J. Phys. Chem B*, submitted for publication.

(31) Umebayashi, T.; Yamaki, T.; Tanaka, S.; Asai, K. *Chem. Lett.* **2003**, *32*, 330.

(32) Umebayashi, T.; Yamaki, T.; Itoh, H.; Asai, K. *Appl. Phys. Lett.* **2002**, *81*, 454.

(33) Lei, Z.; Ma, G.; Liu, M.; You, W.; Yan, H.; Wu, G.; Takata, T.; Hara, M.; Domen, K.; Li, C. *J. Catal.* **2006,** *237*, 322.

(34) Palankowski, V. Ph.D. Thesis, Technical University of Vienna, Austria, December 2000.

(35) Ayalew, T. Ph.D. Thesis, Technical University of Vienna, Austria, January 2004.

(36) Emeline, A. V.; Ryabchuk, V. K.; Serpone, N. *J. Phys. Chem. B,* to be submitted for publication.